Reevaluation of the Dynamic Model for Rotational Diffusion of Thin, Rigid Rods in Semidilute Solution

G. T. Keep and R. Pecora*

Department of Chemistry, Stanford University, Stanford, California 94305.
Received September 11, 1984

ABSTRACT: A geometrical model of the "caging" of thin, rigid rods in semidilute solution is used to find the concentration and length dependences of both the maximum allowed rotation angle and the rotational diffusion coefficient of rods trapped in cages. This model may explain some of the discrepancies which have been found in the past between measurements of rotational diffusion coefficients of rodlike macromolecules and the theoretical predictions of Doi and Edwards. A new concentration dependence of the rotational diffusion coefficient is found that converges with the previously predicted $(CL^3)^{-2}$ dependence of Doi and Edwards only for $CL^3 > \sim 500$. It is further argued that rods in concentrated solution cannot properly be viewed as "caged" unless $CL^3 > \sim 50$.

Introduction

The processing of polymeric materials is of longstanding practical importance. The presence of a solvent makes handling of the material easier as the solution viscosity goes down with decreasing concentration. However, high concentrations of the polymer give more of the desired material and less solvent which may be difficult and costly to eliminate and reprocess. Hence, it is of value to understand the relations between solution content and processing difficulty. The "semidilute" region is of particular interest since it is the concentration region dilute enough to flow but concentrated enough to be worth processing (e.g., several percent by weight). However, it is the concentration region with the most enigmatic characteristics. Theory and experiments are not in accord and observation of the limiting behavior falls short of characterizing the transition regions.

Part of the problem is the intractability of solving the equations of motion for the general case of a collection of particles with arbitrary shape and elastic properties. One of the common simplifying models is the infinitely thin, rigid rod. With no flexibility and no volume to the particles, this is a thermodynamically ideal solution. Nonetheless, the dynamics of rigid rods in semidilute solution have so far defied all attempts at obtaining a quantitatively correct solution. This is because the long molecules stretch across a lot of space and have a high potential for hard-core interaction even at relatively low concentrations. Rods may easily block the motion of their neighbors. Patterns of these blocking rods may occur and decay in solution that influence the local motions. It is the nature of these "patterns" of molecules that we are striving to understand.

Doi and Edwards[1-3] have presented a simple model to qualitatively explain the slowing down of rotational diffusion with increasing concentration of thin rigid rods in solution. They approximated the size of "cages" formed of meshes of rodlike molecules in solution that may trap other rods. These cages are simply the neighboring molecules, each of which blocks some of the pathways available for motion of the reference molecule (called the "test" molecule). If there are enough neighbors, no paths remain open and some other mechanism must be found by which a test rod may execute rotational diffusion. Doi and Edwards argued that a test rod may only rotate within the confines of such a cage until it leaves the cage by translation along its length. Thus, they calculated a value for the rotational diffusion coefficient in which the dependence on number concentration (C) and rod length (L) of the rotational diffusion coefficient (Θ) would be given by

$$\Theta = \Theta_0[\beta/(CL^3)^2] \quad (1)$$

where Θ_0 is the dilute-solution value. The value of β was predicted to be a small constant of order 1. Experiments by many researchers[4-9,24] have, in general, agreed with the concentration and length dependences in eq 1. However, to agree quantitatively, they had to postulate β values of order 1000. Some data even suggested that the predicted effects began at higher concentrations than expected, and thus researchers postulated a concentration offset.

Recent explanations of these discrepancies have rested on molecular flexibility and cage escape times. The most insightful explanations have been proposed by Odijk[10,11] and Odell, Atkins, and Keller.[12,13]

Odijk has explored the case of flexible rods. He argued that even slight flexibility may have drastic effects on the predicted confinement of long, thin macromolecules. This effect becomes important when the supposed confinement angle is smaller than the expected bending of the rod. While in real systems flexibility may be an important factor in determining rotational relaxation times, it is the object of the present work to determine the C and L dependence of Θ in the semidilute region for truly rigid rods.

Odell, Atkins, and Keller[12,13] used computer simulations to show that the caging of rods was not complete at concentrations where significant hindrance was originally predicted. The diffusing rods were presented with an inhomogeneous maze of baffles but were not truly caged. Some route for rotation through 180° was always available at the concentrations that they sampled. In order to answer this observation, we wish to find at what concentrations complete caging does occur and how the cage size and consequently the allowed rotational diffusion vary with concentration.

Also of interest is the work of Frenkel and Maguire[14] in which they performed molecular dynamics simulations of fluids composed of thin, hard, rigid rods in the range $1 < CL^3 < 48$. They found that the Enskog method of finding transport properties (based on solute–solute binary collisions) was good only for $CL^3 < 8$ and deviated for higher CL^3. This marks the concentration at which the time correlations in multibody collisions become important. Because of the slow diffusion of neighboring molecules, regions in space are firmly denied to a test molecule which tries to enter the region more than once. This sort of repeated failure is taken into account when binary collision correlations in time are considered. However, as fewer path options succeed at higher and higher concentration, the unfruitful paths are sampled more and more often before the molecule is able to find a free path for motion. This sort of cooperative effect cannot be properly handled in a binary collision theory and leads to the failure of the Enskog theory observed by Frenkel and Maguire. In this way we can see that the higher the concentration becomes,

0024-9297/85/2218-1167$01.50/0

the more important will be the characteristics and duration of each individual environment the molecule encounters.

Frenkel and Maguire also discuss the inherent differences between their simulations of pure fluids of infinitely thin rods and the case of such rods in a continuum solvent. They suggest that caging is valid in the pure fluid case for $CL^3 > 24$.

Real macromolecular systems can have a significant degree of orientation of their constituents. This could be due to the presence of a liquid crystalline phase, or simply a correlation between the positions or the orientations of the individual molecules due to intermolecular forces. Also, many researchers are interested in flow-induced orientation.[15,16] In this paper, however, we treat only the case of random, isotropic distributions of molecular positions and orientations. Hence, we may take there to be no correlation between any two rods. This greatly simplifies the averaging process. It should, in principle, be possible to generalize this model to the case of a solution of oriented rods, but then the following averages would have to be done with any orientational correlations included explicitly.

Polydispersity is another complicating aspect of real systems which has been addressed in part by Marrucci and Grizzuti.[16] They wrote out detailed expressions for caging given a collection of rod sizes with arbitrary orientational distributions (as generated in a flow), but only in the context of the original Doi–Edwards theory. Their preaveraging approximations used to reduce these equations to a usable form are of general interest, however, as they make use of the fact that the caging contributions of the smaller rods relax away faster than those of the larger rods due to inherently faster motions. This sort of consideration will be important in examining the decay of a cage in real systems.

It also is becoming apparent[17] that the thermodynamic effects on diffusion processes are always present and important in real chemical systems. Long-range forces have big effects when they are present. The role of entanglement-based models is to find what additional kinetic restrictions are placed on the diffusion process.

A simple rotational relaxation process is seen in dilute solutions and would be expected to be unchanged if collisions with other solute molecules were totally uncorrelated in position and time. The effect of entanglements is to change this to a complex, multimodal process. On fast time scales the solute molecules diffuse within the kinetically allowed boundaries or cages that hold them. Any orientational correlation that has persisted then relaxes on slower time scales as the molecules escape the cages or the cages themselves relax their shapes. The reader interested in fast-time behavior within the cage is referred to the restricted rotation in a cone model of Wang and Pecora.[18] It is the slowest relaxation that is of viscomechanical concern. Below, we refer to this slowest relaxation as a "mode" that can be characterized by a "rotational diffusion coefficient" but it must be recognized that this is an oversimplification of a more complex process, whose overall form is not yet fully understood.

Spherical Surface Model

The spherical surface model is illustrated in Figure 1. A test rod is fixed at its center of mass and is allowed random angular orientation. The region swept out by all its possible orientations is a sphere of diameter L. Rotational diffusion will correspond to its ends doing a random walk on the surface of this sphere. A blocking rod that punctures the sphere is depicted in Figure 1a. The segment inside the sphere blocks the test rod's rotation. This

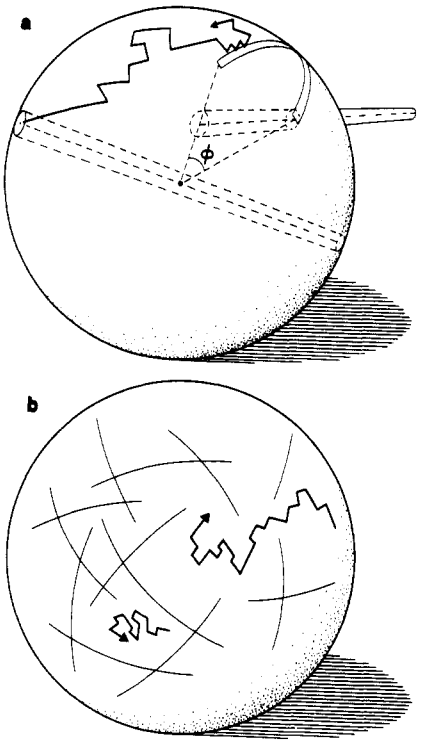

Figure 1. (a) The tip of a test rod does a random walk on the surface of a sphere. A blocking rod punctures the sphere and casts an uncrossable shadow of arc angle ϕ. (b) A collection of these arcs on the surface of the sphere form channels or even cages from which the tip of the test rod may not escape.

is equivalent to saying that this intruding segment's "shadow" (as cast by a light source at the center of mass of the test rod, cast onto the surface of the sphere) blocks the random walk of the *tip* of the test rod on this surface. All of the intruding segments may be viewed this way in terms of their effect on the motion of the *tip* of the test rod. We can calculate some of the expected characteristics of these shadows including their size distribution and average number. With this information, we will proceed to calculate the characteristics of the cages they form on the surface of the sphere (see Figure 1b) that trap the test rod and prevent it from rotating freely. To begin, we must realize that these shadows will be arcs of great circles of the sphere. Thus, we can characterize them simply with a point, a direction, and a length of arc angle ϕ.

The first step in treating this model is to calculate the number and average size of these arcs as a function of rod length (L) and number concentration (C). We will then look at their intersections which build up in number with concentration in a nonlinear fashion to form cage regions. The cage may be used as the boundary of the fast-time motions. We will also proceed to estimate the slow-time rotational diffusion coefficient by combining this result with an estimated cage escape time.

We now proceed using the construct in Figure 2. This is a cross section of a solid of revolution, symmetric about the Z axis of a cylindrical coordinate system. The center of mass of the test rod is fixed at the origin, which is at the center of the diagram. It is allowed random angular orientation and sweeps out the region given by the dark inner sphere. The blocking rod is then defined to lie parallel to the Z axis with center of mass coordinate z and radial coordinate r. The angle α defines the direction that the blocking rod is offset from the Z axis, although it only enters the calculation via a volume element. The outer perimeter of the construct designates the volume in which the blocking rod's center of mass must lie in order to

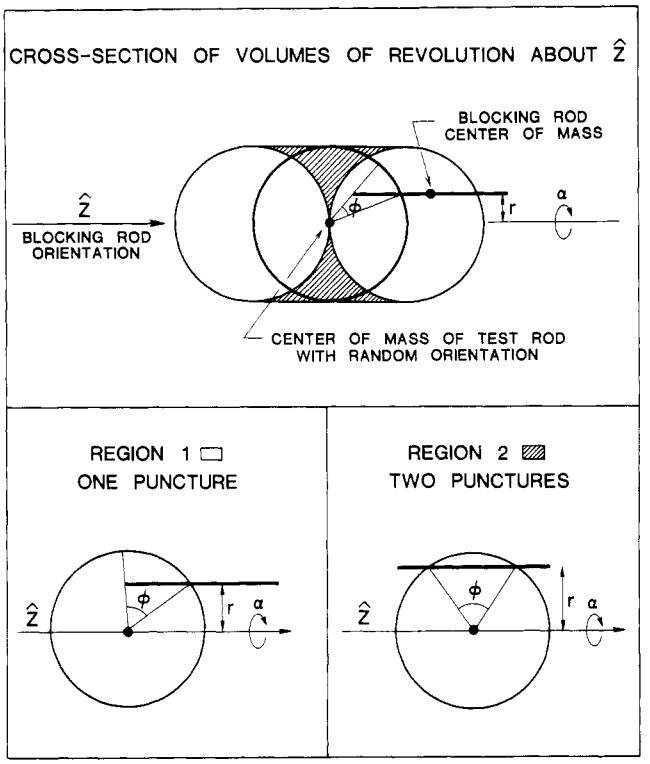

Figure 2. Top: Cross section of region surrounding the center of mass of the test rod. The region is cylindrically symmetric around the Z axis. If the blocking rod lies in this region, it punctures the test rod's enveloping sphere either once or (in the shaded region) twice. The Z axis defines the orientation of the blocking rod; the rotating rod has random orientation. Bottom: Arc definitions corresponding to center of mass of the blocking rod in each of the two shaded regions in the top panel.

puncture the test rod's enveloping sphere at least once. If the blocking rod center of mass is in the shaded volume, the rod punctures the surface of the test rod's enveloping sphere twice.

Multiplying the total volume (which corresponds to any punctures at all and is in the shape of a spherocylinder) by the number concentration yields that the average number of rods that puncture the center sphere and hence could restrict the test rod's motion is

$$\langle N \rangle = (5\pi/12)CL^3 \tag{2}$$

This is identical with the average number of rods that come within a distance $L/2$ of the center of mass of the test rod.

Also from the relative volumes of the shaded and nonshaded volumes of revolution we can see that 4 times as many rods puncture the central sphere once as do so twice. In other words, $^1/_5$ of the rods that come within $L/2$ of the center of mass of the test rod do so only with a central portion of their length and not with either end.

We now find the average arc angle ϕ. This averaging is done via an integral over all possible coordinates of the blocking rod. This can be simplified by using trigonometric arguments that yield arc angles averaged over z and α. This leaves ϕ to be a function of radius r only for two different cases.

Case 1. Single Puncture. (See Figure 2, lower left corner.) For a given distance from the blocking rod to the z axis, r, symmetry gives for the average over possible z coordinates

$$\langle \phi \rangle(r) = \cos^{-1}(2r/L) \tag{3}$$

with a frequency of occurrence

$$\text{weight} = r\,dr\,[(L/2)^2 - r^2]^{1/2} \tag{4}$$

(the range of z positions giving rise to one puncture). So

$$\langle \phi \rangle_1 = \frac{\int_{r=0}^{L/2} r\,dr\,[(L/2)^2 - r^2]^{1/2} \cos^{-1}(2r/L)}{\int_{r=0}^{L/2} r\,dr\,[(L/2)^2 - r^2]^{1/2}} = \pi/2 - {}^2/_3 \tag{5}$$

Case 2. Double Puncture. (See Figure 2, lower right corner.) For a given r

$$\phi(r) = 2\cos^{-1}(2r/L) \tag{6}$$

with a frequency of occurrence

$$\text{weight} = L - 2[(L/2)^2 - r^2]^{1/2} \tag{7}$$

(the range of z positions giving rise to two punctures).

$$\langle \phi \rangle_2 = \frac{\int_{r=0}^{L/2} r\,dr\,(L - 2[(L/2)^2 - r^2]^{1/2})(2\cos^{-1}(2r/L))}{\int_{r=0}^{L/2} r\,dr\,(L - 2[(L/2)^2 - r^2]^{1/2})} = {}^8/_3 - \pi/2 \tag{8}$$

Finally, from the relative frequency of occurrence of the two cases, we have

$$\langle \phi \rangle = {}^4/_5\langle \phi \rangle_1 + {}^1/_5\langle \phi \rangle_2 = 3\pi/10 \tag{9}$$

These arcs are here assumed to be distributed randomly in the laboratory frame of reference. Our next step is to find the number of intersections these arcs form. To do this the following point must be noted; the test rod has two ends, either of which may be blocked by a blocking rod. If we wish to view the rod's rotational diffusion as the random walk of a *single* point on the sphere surface, we must then view each blocking arc as having an identical twin arc on the opposite side of the sphere. Hence, each time an arc intersects another arc, or its twin, two intersections are formed which may serve as corners of cages. If such occurs, the intersections formed will be at the two intersections of the great circles in which the arcs lie. This pair of intersections will occur if both arcs fall across either of these two points. This dual intersection has a joint probability of occurring, P, for two random arcs

$$P = \left\langle \frac{\phi_i}{\pi} \frac{\phi_j}{\pi} \right\rangle = \frac{\langle \phi \rangle^2}{\pi^2} = \frac{9}{100} \tag{10}$$

The number of possible intersections of arcs is the number of ways of taking two arcs from the N available; hence, the average total number of intersections of arcs and twins on the sphere surface is

$$\text{no. of intersections} = {}^1/_2 N(N-1)(P)(2) \tag{11}$$

With the above equations it is now possible to make some remarks about the concentrations at which true caging sets in. Caging is exceedingly unlikely until the number of intersections at least equals the number of arcs plus twins. This is the number of intersections it takes to tie all the arcs together into one big network if they are tied together in the most efficient manner possible. The concentration at which this is expected to happen can be found by setting the number of intersections equal to $2N$, which gives $CL^3 = 17.7$. This concentration would permit the formation of one large ring (end-to-end or with pendent arms) that would divide the sphere into two regions (cages). Formation of more cages would be at the expense of leaving some arcs floating unconnected. Clearly, at this concentration some cages will form but the bulk of the sphere

surface will be fairly easily accessible through rotation of the test rod. An average of two intersections per arc would occur at a concentration of $CL^3 = 34.7$. Hence one would expect predominantly cages, but perhaps with a few channels remaining, mazelike, between groups of interconnecting arcs. An analytical analysis of the stochastic fluctuations which could give rise to these open channels has not been done, though there is some similarity between this problem and polymerization statistics in the presence of excessive cyclization.

Consider now the effect of adding an arc to an existing collection of intersecting arcs already drawn on the surface of a sphere. As the new arc is drawn in, each new intersection formed is followed by cutting an existing cage in two, except for the cage entered after the last intersection is drawn. Thus, the number of cages expected is equal to the number of intersections minus the number of arcs and twins. An additional one should be added since with no blocking rods there is one, not zero, cages (i.e., all space). Also a variable should be added which equals the number of groups of interlocking shadows between which groups there are no connecting intersections. This effect increases the number of cages present by one for each separate network. However, simulations performed by drawing arcs on a rubber ball with a felt-tipped pen suggest that all of the arcs are interconnected at concentrations above about $CL^3 = 50$. Thus, these correction factors will only have a value of +2 above $CL^3 = 50$, which is 1% of the cages at $CL^3 = 50$. Thus, we may make the approximation that

$$\text{no. of cages} = N(N-1)P - 2N$$
$$(\text{error} < 1\% \text{ for } CL^3 \geq 50) \qquad (12)$$

Below this concentration, when the correction factor will be larger than +2 cages, we have, by definition, independent groups of networks. This means that there are free channels between these groups and hence caging is not the universal case. This shows that caging theories are not valid and a diffusion-in-a-maze model must be used. Therefore, a more precise equation for the number of cages for low concentration would be fundamentally suspect. Note, however, that this approximation is the cause of the catastrophic divergence of the final equation (eq 23) in the dilute-solution limit. The fact that we are forced to ignore the question of independent networks below $CL^3 = 50$ is integrally linked to the difficulty of finding the point of complete caging. Unfortunately, these remain unresolved.

In summary, we expect complete caging to occur within 50% of the second concentration above, or somewhere in the range $20 < CL^3 < 50$, and have confidence in the caging concept only above these concentrations.

We now have in eq 12 an expression for the number of cages which surround the center of mass of the test rod, in one of which the rod will find itself temporarily trapped. The area of the sphere on which the ends of the test rod will be found (by definition) will be divided up among these cages, giving the average area per cage as

$$\langle \text{area} \rangle = \frac{4\pi(L/2)^2}{N(N-1)P - 2N} = \frac{\pi L^2}{P(N^2 - N(1 + 2/P))} \qquad (13)$$

or for the average solid angle subtended by the cage we get, with the aid of eq 2, 10, and 13

$$\langle \Omega \rangle = \langle \text{area} \rangle / (L/2)^2$$
$$= 4\pi/P(N^2 - N(1 + 2/P))$$
$$= 400\pi/9(N^2 - (209/9)N)$$
$$= 256/\pi((CL^3)^2 - (836/15\pi)CL^3) \qquad (14)$$

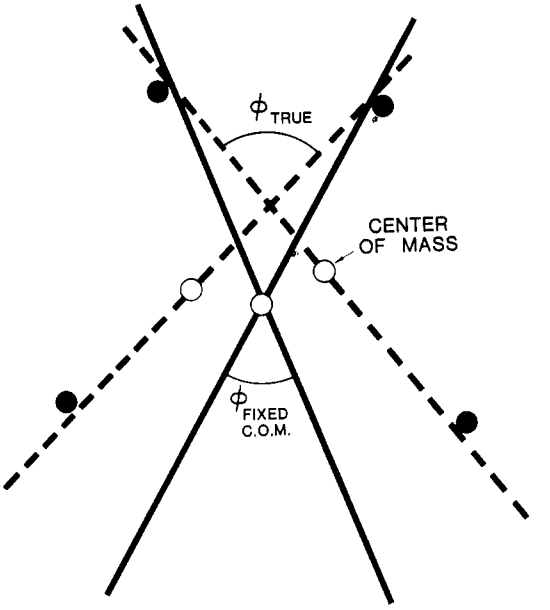

Figure 3. An example of a case where fixing the center of mass unreasonably restricts the rotation of a "caged" rod.

We must further consider that a diffusing rod will not be expected to enter and leave its cage along the boundary walls thus taking full advantage of the allowed rotation. Rather it would enter and leave somewhere within these limits. It can be shown that for random entry and exit points from a square region

$$\langle \theta^2 \rangle = \langle \Omega \rangle / 3 \qquad (15)$$

where $\langle \theta^2 \rangle$ is the average-square angle of rotation. The exact numerical relation in eq 15 depends weakly on the shape of the caging region. In the high-concentration limit, the cages are expected to be convex polygons with an average of four sides per cage, so the result for a square cage cross section is used here. In highly oriented solutions, the cages might be expected to be long and thin and the high anisotropy of the cages (in shape and orientation) would have to be considered in more detail. This suggests, for instance, that rotation around the axis of common orientation (for a rod out of alignment) would be harder than rotation away from this axis.

The limit of our analytic results is thus

$$\langle \theta^2 \rangle = 256/3\pi((CL^3)^2 - (836/15\pi)CL^3) \qquad (16)$$

for isotropic distributions and high enough CL^3. Note that we have also allowed for only pure rotation.

Center of Mass Constraint

A major deficiency in the above model is that the center of mass of the test rod is taken fixed such that the limit of an allowed rotation is determined by one end of the test rod and the center of mass. Instead, the center of mass should be allowed slight shifts such that the limit of rotation is defined by the two ends (see Figure 3). The release of this constraint would be expected to give a larger value of $\langle \theta^2 \rangle$. This accounts for the effect of molecular translation perpendicular to the rod axis which in past theories has been set identically equal to zero.

A second factor we have not considered is the complete effect of fluctuations of the local blocking rod density on their caging ability. This should affect the averaging process.

In order to address these problems, we resorted to some simple Monte Carlo simulations. For ease of calculation, these were done by using only one degree of rotational

freedom. This puts the test rod rotating in a plane while blocking rods become blocking points at their intersections with the plane of rotation. Their average number as a function of concentration may be easily calculated analytically. The quantity of interest is the ratio of the allowed rotational angle found without fixing the center of mass to that found with the center of mass fixed. This ratio is used as a scale factor for each of the two rotational degrees of freedom in the earlier equations.

The only difficult part of this simulation was finding the limit of rotation with the center of mass free. This was done as follows. Proposed rotations were sampled in smaller and smaller steps to find the largest angle that was allowed. A rotation was "allowed" if, when coupled with an appropriate translation perpendicular to the rod axis, the test rod did not pass through any blocking points. This condition was tested by finding the Cartesian coordinates of the blocking points in a frame of reference aligned with the proposed rod orientation. The order of the coordinates perpendicular to the new rod axis would tell us if the rod could have the new orientation and still be between the two original groups of blocking points on the two sides of the rod.

The minimum concentration at which this calculation could be performed was about $CL^3 = 30$ since below this point some environments generated did not prevent the test rod from leaving the space allotted to the simulation. This corresponds to 10–12 blocking points in a circle of diameter L.

The calculations presented here were done on a Charles River Data System's Universe 68 with floating point processor. One thousand cages could be sampled and resolved to 1 part in 100 000 in approximately 1 h for $CL^3 = 150$. This degree of precision was used on each of the blocking point densities examined which was increased incrementally. The speed was highly dependent on the density of blocking rods.

The quantity of interest is the ratio of true maximum allowed rotational angle to that predicted with a fixed center of mass. Each of these quantities is plotted separately vs. concentration in Figure 4a. In Figure 4b are the distributions of angle sizes for both fixed and free center of mass for a typical concentration. This ratio occurred in a highly skewed distribution making the properly weighted result give far different results from an averaging process which weights each cage equally no matter how small. When averaged properly (weighting each cage's contribution by its corresponding probability of being occupied), no concentration dependence to the ratio was seen. The ratio of the averaged quantities was 1.79 ± 0.05 while the average of the ratio for each cage was 2.50 ± 0.06. It is the latter quantity which must be introduced as a correction factor for each of the two degrees of rotational freedom. This modifies eq 16 to give eq 17 as a master equation for the average rotation executed within a single cage.

$$\langle\theta^2\rangle = \frac{(2.50)^2(256)}{3\pi((CL^3)^2 - (836/15\pi)CL^3)} \tag{17}$$

Cage Escape Times

Controversy surrounds the question of the transition time from one cage to the next. The average time corresponding to a complete longitudinal displacement of one rod length in either direction

$$\langle t\rangle = L^2/2D_\parallel \tag{18}$$

is an upper bound to the cage escape time. A more justifiable choice for escape time is that for which the excursions in both directions along the rod sum to the rod length (L) since this allows a constraint on the rod to "slip around" one end or the other. Numerical calculations give

$$\langle t\rangle = L^2/3D_\parallel \tag{19}$$

If we include the idea of a fixed fraction (f) of the rod length that the excursions must sum to (or a fraction of the constraints that must be evaded) for a new cage to manifest, we get the final result

$$\langle t\rangle = (fL)^2/3D_\parallel \tag{20}$$

Clearly $f < 1$ since the caging rods are themselves moving and may "slip around" the test rod. Also, not *all* of the constraints need to be removed for a path to open which allows the test rod to rotate into a new region, wholly or little by little. We find later that for the final equation for the rotational diffusion coefficient (eq 23) to be consistent with the above observation that the concentration at which complete caging occurs must be between $CL^3 = 20$ and $CL^3 = 50$, we must have $1.5 < f^{-1} < 8.7$. Our best guess from available experimental data[4-9,24] is $f \sim {}^1/_6$. This may be a function of flexibility or other variables in the experiments, perhaps even CL^3.

It is worthwhile to mention at this point that for systems for polydisperse rods, the dynamics of blocking rods of different length could become quite complicated. The ideas of Marrucci and Grizzuti[16] mentioned in the introduction might prove useful in treating this case. Even for

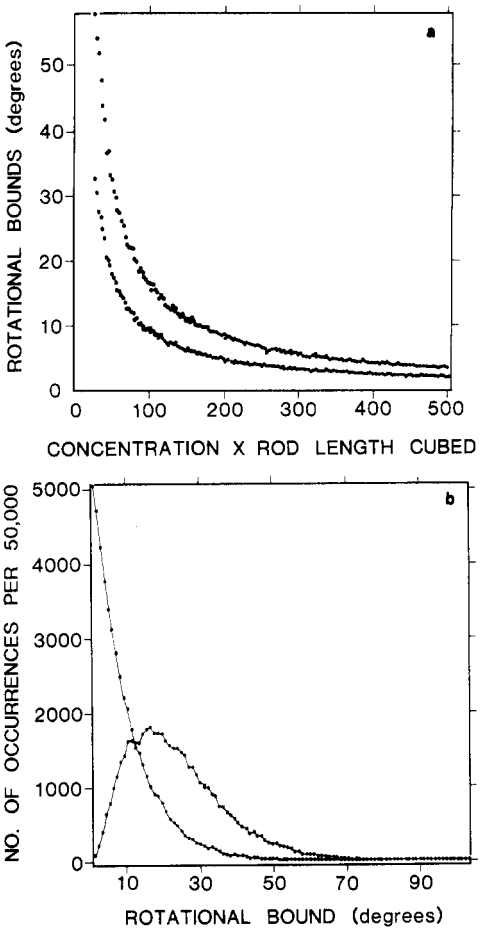

Figure 4. Some sample Monte Carlo results: (a) Average rod rotation limits in a plane as a function of CL^3. The top curve is the true rotational mobility while the bottom is that predicted with center of mass fixed. (b) The distributions of the above angles at a fixed concentration; $CL^3 = 51$. The monotonic distribution is with center of mass fixed—the humped distribution is for a free center of mass.

the case of monodisperse rods, there is a correlation between the size of the blocking arc a rod presents and the ease with which its contribution relaxes, as can be seen from the model presented here. (Example: A broad shallow penetration of the sphere enveloping a test rod, by a blocking rod, is among the longest blocking arcs, yet the easiest to remove from the sphere.) These factors complicate a description of relaxation of the cage itself, but may be treated in similar fashion to the polydispersity.

Using the original Broersma relations for long, thin rods[19-22] in the limit $L/d \rightarrow \infty$

$$D_{\parallel} = (kT/2\pi\eta L) \ln (L/d)$$

$$\Theta_0 = (3kT/\pi\eta L^3) \ln (L/d)$$

$$D_{\parallel} = \Theta_0(L^2/6) \tag{21}$$

and the definition of the rotational diffusion coefficient with two angular degrees of freedom

$$\Theta = \langle\theta^2\rangle/4t \tag{22}$$

along with eq 17 above, we get a combined result for the rotational diffusion coefficient

$$\frac{\Theta}{\Theta_0} = \frac{(2.50)^2(32)}{3\pi f^2((CL^3)^2 - (836/15\pi)CL^3)} \tag{23}$$

This equation crosses the $\Theta_0/\Theta = 1$ axis at a concentration dependent on the choice of f. Below this concentration the equation does *not* give meaningful results. This is due in part to the validity of the model but also because, below this concentration, the *allowed* rotations in some cages are greater than the rod would normally execute before leaving the cage, leading to a prediction of a larger *allowed* rotation than actually takes place. Hence, below this concentration, the average cage presents no significant barrier to rotation, being larger than the actual diffusive paths taken. However, since there is expected to be a distribution of cage sizes, some attempted rotations even below this concentration will be caged by the smallest cages of the existing distribution. Hence, a proper averaging over cage sizes with a cutoff for large cages would be expected to make the curve level off smoothly at $\Theta_0/\Theta = 1$. This has not been done since the cage model should likely give way to a diffusion-in-a-maze model for this region. Hence, our result mainly shows that, for several reasons, caging concepts are best not applied to such low concentrations (i.e., $CL^3 < 50$).

In Figure 5 is plotted ln (Θ_0/Θ) vs. ln (CL^3) for $f = {}^1/_6$. Also shown is the Doi–Edwards equation with $\beta = 1$ and $\beta = 764$, which our function approaches asymptotically and converges with for $CL^3 > 500$. The dots are the previously reported work of Zero and Pecora[6] which show a leveling off at high concentration as noted by Odijk.[10] This he attributed to the flexibility of the molecules. If this is the case, these data support the hypothesis that eq 23 with $f = {}^1/_6$ would be the rigid rod limit of a family of curves obtained by varying a parameter given by the ratio of the contour length to persistence length. This flexibility parameter is simply the number of persistence lengths comprising the molecule, each of which segments has a certain standardized average expected bend. Effects due to finite diameter and polydispersity have of course been ignored in this model.

Final Discussion

We have found a more detailed expression for the concentration dependence of the rotational diffusion coefficient for concentrated solutions of completely rigid rods than has been obtained in the past. The unexpectedly large values of the rotational diffusion coefficient found by experiment may in this fashion be partially explained on the basis of geometry even in the absence of flexibility. In particular the onset of semidilute entanglement at a concentration much higher than $CL^3 = 1$ (which is usually quoted as the lower limit of the semidilute region) is explained by considering the statistics of cage formation instead of just the limiting scaling behavior. The effects caused by flexibility and thickness are not accounted for by this theory.

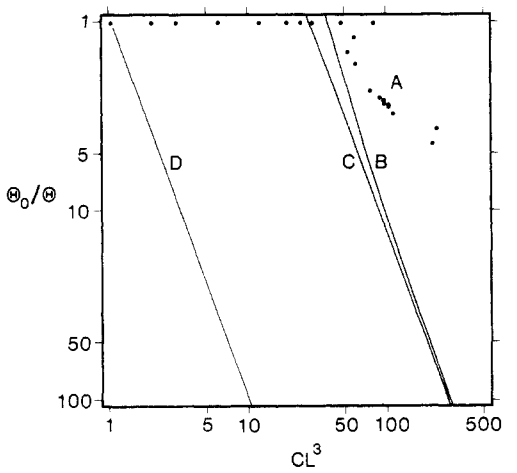

Figure 5. Plot of Θ_0/Θ vs. CL^3 on log scales. (A) The dots are previously reported experimental data of Zero and Pecora (ref 6) on three molecular weights of poly(γ-benzyl L-glutamate) (which virtually superimpose on each other) which shows a leveling off trend—probably due to finite flexibility. (B) Equation 23 with $f = {}^1/_6$. (C) Doi and Edwards equation with $\beta = 764$, which matches the high-C limit of curve B. (D) Doi and Edwards equation with $\beta = 1$.

The new functional form for the rotational diffusion coefficient is given in eq 23 and does not converge with the high-concentration fit to the Doi and Edwards equation until around $CL^3 = 500$. In the process, we have found that the model of a rod being confined to a cage which prevents rotation until the rod leaves the cage cannot possibly be valid below $CL^3 = 17.7$ and can only be relied upon at this level of approximation above $CL^3 = 50$.

Unfortunately, direct comparison with most published work is difficult since these results are often parameterized under the unfounded assumption that Θ scales as a simple power of C (i.e., that a log–log plot is necessarily linear in the region of most interest). Also, the interesting crossover region is often deliberately ignored since it shows the strongest deviations from the simple scaling "laws".

The complexities which surround studies of rodlike macromolecules in the "semidilute" region are beginning to become manifest. On the low end of the concentration scale, rods are incompletely caged and must be viewed, instead, as being caught in a maze of baffles, as envisioned by Odell, Atkins, and Keller. On the high end of the concentration scale, "log jamming effects"[23] (from end-on collisions) and an anticipated transition to a liquid crystalline phase invalidate this model which assumes infinitely thin rigid rods in this concentration region. More importantly, as realized by Odjik, the existence of even slight flexibility in real systems will have a marked effect beyond a certain concentration, tending to level off the rotational diffusion coefficient as C increases.

In the limit of thin, rigid rods, the second virial coefficient is zero and we can divide the concentration scale into several regions: $0 < CL^3 < 1$ dilute solution—short-range interactions may be ignored; $1 < CL^3 < 10$ Enskog-type binary collision theories valid—multiparticle correlations

through time may be ignored; $10 < CL^3 < 50$ current theories inadequate—diffusion in a maze with cages appearing and disappearing with time; $50 < CL^3 < 500$ caging theories reasonable; $500 < CL^3$ Doi and Edwards dependence valid for infinitely thin rigid rods.

Generalization of the averages done in this paper to anisotropic solutions is expected to be complex but would be of immense value since a flowing system will be partially aligned by the flow. An incorporation of the effects of flexibility, polydispersity, and finite thickness of the molecules should also be of interest in treating the case of real physical molecules. Experimental work is needed especially in finding the variation in behavior with the flexibility parameter.

Also, the onset of semidilute behavior should be sought and characterized in the region $20 < CL^3 < 50$ by either experimental methods or by dynamic modeling of cage rearrangement, or both.

Acknowledgment. This work was supported by the NSF-MRL Program through the Center of Materials Research at Stanford University and NSF Grant CHE-82-00512.

References and Notes

(1) Doi, M. *J. Phys.* (*Paris*) **1975**, *36*, 607.
(2) Doi, M.; Edwards, S. F. *J. Chem. Soc., Faraday Trans. 2* **1978**, *74*, 560.
(3) Doi, M.; Edwards, S. F. *J. Chem. Soc., Faraday Trans. 2* **1978**, *74*, 918.
(4) Southwick, J. G.; Jamieson, A. M.; Blackwell, J. *Macromolecules* **1981**, *14*, 1728.
(5) Doi, M. *J. Polym. Sci., Polym. Phys. Ed.* **1981**, *19*, 229.
(6) Zero, K.; Pecora, R. *Macromolecules* **1982**, *15*, 87.
(7) Maguire, J. F. *J. Chem. Soc., Faraday Trans. 2* **1981**, *77*, 513.
(8) Mori, Y.; Ookubo, N.; Hayakawa, R.; Wada, Y. *J. Polym. Sci., Polym. Phys. Ed.* **1982**, *20*, 2111.
(9) Brown, W. *Macromolecules* **1984**, *17*, 66.
(10) Odijk, T. *Macromolecules* **1983**, *16*, 1340.
(11) Odijk, T. *Macromolecules* **1984**, *17*, 502.
(12) Odell, J. A.; Atkins, E. D. T.; Keller, A. *J. Polym. Sci., Polym. Lett. Ed.* **1983**, *21*, 289.
(13) Expanded version of ref 12 submitted to *Pure Appl. Chem.*
(14) Frenkel, D.; Maguire, J. F. *Phys. Rev. Lett.* **1981**, *47*, 1025 and expanded in *Mol. Phys.* **1983**, *49*, 503.
(15) Chow, A. W.; Fuller, G. G. *Macromolecules* **1985**, *18*, 786. Chow, A. W.; Fuller, G. G.; Wallace, D. G.; Madri, J. A. *Macromolecules* **1985**, *18*, 793, 805.
(16) Marrucci, G.; Grizzuti, N. *J. Polym. Sci., Polym. Lett. Ed.* **1983**, *21*, 83.
(17) Russo, P. S.; Langley, K. H.; Karasz, F. E. *J. Chem. Phys.* **1984**, *80*, 5312.
(18) Wang, C.-C.; Pecora, R. *J. Chem. Phys.* **1980**, *72*, 5333.
(19) Broersma, S. *J. Chem. Phys.* **1960**, *32*, 1626.
(20) Broersma, S. *J. Chem. Phys.* **1960**, *32*, 1632.
(21) Newman, J.; Swinney, H. L.; Day, L. A. *J. Mol. Biol.* **1977**, *116*, 593.
(22) Broersma, S. *J. Chem. Phys.* **1981**, *74*, 6989.
(23) Edwards, S. F.; Evans, K. E. *J. Chem. Soc., Faraday Trans. 2* **1982**, *78*, 113.
(24) Statman, D.; Chu, B. *Macromolecules* **1984**, *17*, 1537.

Concentration-Dependent Translational Friction Coefficients of Polymers with Excluded Volume Effect in Dilute Solutions

Mark DeMeuse

Department of Chemistry, Illinois Institute of Technology, Chicago, Illinois 60616

M. Muthukumar*†

Polymer Science and Engineering Department, University of Massachusetts, Amherst, Massachusetts 01003. *Received September 7, 1984*

ABSTRACT: Using a multiple scattering approach, we obtain explicit expressions for the leading concentration dependence of self-friction and cooperative translational friction coefficients of a flexible polymer chain with arbitrary excluded volume interaction. Employing Fixman's radial distribution function for the polymer chains, we find $k_s/[\eta]$ for the self-friction coefficient to change smoothly from 0.75 at Θ temperature to 0.45 in very good solutions, while for the cooperative friction coefficient the corresponding change is from 0.75 to 1.85. Comparison of our calculated results with the available experimental data is also presented.

I. Introduction

The translational friction coefficient, f_t, of a polymer molecule in dilute solutions at a concentration c is given by

$$f_t = f_t^{(0)}(1 + k_s c + ...) \tag{1.1}$$

where $f_t^{(0)}$ is the infinite-dilution friction coefficient. Experimentally both $f_t^{(0)}$ and k_s, which are used to characterize the polymers, are easily obtainable quantities as the intercept and the initial slope, respectively, of a plot of f_t vs. c. The calculation of $f_t^{(0)}$ of an isolated flexible chain in a hydrodynamic medium is a well-understood old problem and is reviewed in the literature.[1,2] When many chains are present, the intrachain hydrodynamic interaction is considerably modified.[3-5] Due to the long-ranged nature of the hydrodynamic interaction, the calculation of the extent of this modification and the value of k_s is not straightforward and has attracted considerable interest.[3-11]

There have been many previous attempts in the literature to calculate k_s. Yamakawa,[6] by assuming that the polymers obey random-flight statistics, has provided an extension of the Kirkwood–Riseman theory for $f_t^{(0)}$. The resulting formula predicts $k_s = 0.2[\eta]$ at the Θ temperature, where $[\eta]$ is the intrinsic viscosity. A formula for extrapolating to the good-solution limit is provided in terms of A_2, the second virial coefficient. Unfortunately, reliance on existing experimental data is needed to obtain the dependence of k_s on the solvent quality. Pyun and Fixman[7] treated the problem for interpenetrable spheres. They obtained $k_s = 0.45[\eta]$ under Θ conditions. They also provide an extrapolation formula to the hard-sphere limit, which is assumed to correspond to the good-solvent case. Following Pyun and Fixman's work, there have been numerous investigations[8] reported in the literature to calculate k_s for a suspension of spheres. The most important

† Alfred P. Sloan Research Fellow.

0024-9297/85/2218-1173$01.50/0